

REVIEW OF FATIGUE AND FRACTURE RESEARCH AT
NASA LANGLEY RESEARCH CENTER

R. A. Everett, Jr.

U.S. Army Aerostructures Directorate, ARTA (AVSCOM)
NASA Langley Research Center

Most dynamic components in helicopters are designed with a safe-life, constant-amplitude testing approach that has not changed in many years. In contrast, the fatigue methodology in other industries has advanced significantly in the last two decades. Perhaps the helicopter industry should take a closer look at design methodology in other industries and at recent research findings to see if changes in their design methodology are warranted. The purpose of the current paper is to review recent research at the NASA Langley Research Center and U.S. Army Aerostructures Directorate at Langley relating to fatigue and fracture design methodology for metallic components. Most of the Langley research has been directed towards the damage tolerance design approach, but some work has been done that is applicable to the safe-life approach. The research areas to be discussed are identified in the following two paragraphs.

In the area of testing, damage tolerance concepts are concentrating on the "small-crack" effect in crack growth and the measurement of crack opening stresses. Current safe-life test programs pertain to developing correction factors to Miner's rule to account for the damage caused by ground-air-ground load cycles and using the local strain approach for determining fatigue life. Tests have also been conducted to determine the effects of a machining scratch on the fatigue life of a high strength steel.

In the area of analysis, work is concentrated on developing a crack closure model that will predict fatigue life under spectrum loading for several different metal alloys including a high strength steel that is often used in the dynamic components of helicopters. Work is also continuing in developing a three-dimensional, finite-element stress analysis for cracked and uncracked structures, as well as developing a boundary element method for cracked isotropic and anisotropic structures. A numerical technique for solving simultaneous equations called the multigrid method is being pursued to enhance the solution schemes in both finite-element analysis and boundary element analysis. Finally, a fracture mechanics project involving an elastic-plastic finite element analysis of the J-resistance curve is also being pursued.

Under the two major headings of testing and analysis, each of the above topics will be briefly discussed.

TESTING

Small-Crack Effect

The possibility of a "small-crack" effect in the crack growth process in metals was first revealed when Pearson (ref. 1) published his paper on the growth of very short cracks in aluminum alloys in 1971. In his work, he showed that the linear elastic stress intensity range(ΔK) did not correlate crack growth rate data for very small cracks(6 to 500 μm). In fact, his data showed that for the same ΔK values the so-called "small cracks" propagated at a much faster rate than the large cracks. Today, some researchers believe that this is an area where fracture mechanics breaks down and that a probabilistic approach using stress as a correlating factor is the best approach (ref. 2 and 3). However, other researchers believe that it just takes a proper analysis of this problem for fracture mechanics to work.

At NASA Langley, work has been done showing the effectiveness of fracture mechanics in the "small crack" regime with 2024-T3 aluminum alloy(ref. 4). The testing portion of this work has monitored the initiation and growth of small cracks(5 to 500 μm) at a semi-circular notch in 2024-T3 under constant-amplitude loading at a stress ratio of -1. Typical results from these tests are shown in figure 1 where data is presented in the form of crack growth rates versus ΔK for cyclic tests at a maximum gross stress of 80 MPa. As stated previously, these data show that at a given value of ΔK , crack growth rates for small cracks are much faster than the large crack data represented by the dashed line. The solid line in this figure represents an analytical prediction of these data calculated from a crack growth model developed by Newman(ref. 5). The Newman model uses large-crack growth rate data that has been adjusted to account for the effects of crack closure. In using this model to predict growth rates in the short-crack regime, the large-crack threshold behavior was ignored and an effective ΔK threshold behavior was defined as shown by the dash-dot line in Figure 1 (ref. 4). From photomicrographs, crack initiation was viewed to generally occur at inclusion particle clusters. These cracks appear to have initiated from defects caused by the separation of the alloy matrix material from an inclusion cluster(ref. 4).

Further tests generated life-to-failure data for constant-amplitude loading at stress ratios of -2,0, and 0.5 as well as under spectrum loading. Figure 2 shows the results at a stress ratio of 0.5 and the prediction made by the crack closure model of Newman. Very good agreement is shown between the experimental data and the analytical predictions.

Finally, in figure 3 experimental life-to-failure data generated under a fighter spectrum called FALSTAFF (ref. 6) shows good agreement for loading conditions that are more like an aircraft would experience. Again the solid curve is the life prediction made by the crack closure model (ref. 5).

The small-crack effect is also presently being studied using 4340 steel and 7075-T6 aluminum alloy. In the test program on 4340 steel, a helicopter load spectrum known as HELIX(ref. 7) is being used to generate crack growth data for loads more like the actual loading environment experienced by a hinged rotor helicopter. Study of the small-crack effect

in metals has a potentially large payoff, in that the fatigue process is being examined in the crack length regime where components spend most of their fatigue life.

Crack Opening Stress Measurements

In the study of crack growth in metallic structures, concepts from fracture mechanics have become the principle tools for analyzing cracked configurations. The use of concepts like stress intensity factors from fracture mechanics were first used to describe the behavior of fatigue crack growth when a fatigue crack was modeled by a zero-width saw cut. An elastoplastic analysis by Rice(ref. 8) of this idealised crack under cyclic tensile loading showed that the crack would not be fully closed upon unloading until the applied load was zero. However, experimental work by Elber(refs. 9 and 10) showed that a fatigue crack under cyclic loading would close upon unloading before the applied load reached zero. The stress level at which the crack will proceed to grow again is called the crack opening stress and is often different than zero. These crack opening stresses can be determined by experimental measurements and it is these measurements which are generally believed to be essential in the process of crack growth predictions(ref. 11). The crack opening stress is used in the calculation of the effective stress intensity range, ΔK_{eff} , which is believed to be the appropriate parameter for correlating crack growth rates under various loading conditions. An excellence review paper on fatigue crack closure by Schijve is given in reference 11.

In the determination of the large-crack stress intensity threshold, ΔK_{th} , it has been shown that ΔK_{th} is a function of the material and other test variables, the most significant of these being the stress ratio, R , and the environment(ref. 12). Previous work(ref. 13 and 14) has shown that this R dependency of ΔK_{th} is dramatically reduced if ΔK_{eff} is used as the appropriate concept of the stress intensity range. Recent tests at NASA Langley by Phillips(ref. 12) were conducted to evaluate the capability of ΔK_{eff} to correlate the large-crack stress intensity threshold using crack opening measurements to define ΔK_{eff} .

In these tests, near-threshold crack growth rates were generated using a manually-controlled, discrete-step load shedding method. In this method, after every increment of crack growth of 0.5 mm, the load was reduced by a fixed percentage of the previous value. The percentage load reductions were 6, 18, and 30 percent. These tests were conducted at stress ratios over a range of -2 to 0.7. Figure 4 shows the crack growth rate plotted against ΔK for several R values using the 6 percent load step reduction procedure. These data show the expected dependency of growth rates on R . In order to use ΔK_{eff} as the correlating parameter, opening loads were determined from load-displacement plots using a "reduced displacement" method(ref. 15). These data are shown in figure 5 as a function of the maximum fatigue cyclic load. When the data in figure 4 are replotted using ΔK_{eff} which is determined from the opening stress, the

data as shown in figure 6 do not show the systematic layering with R. The data in this figure also show a smaller scatter for ΔK . The difference in the capabilities of ΔK and ΔK_{eff} to correlate the threshold data is shown quite clearly in figure 7, where ΔK_{th} is plotted against the stress ratio. The $\Delta K_{eff_{th}}$ values are shown by the cross symbols which show a very small variation with R, whereas the square symbols which represent the ΔK_{th} values without stress opening considerations show an obvious dependency on R. In future tests the scatter in the measurements of the opening loads must be kept to a minimum in order to show the true capability of ΔK_{eff} in correlating crack growth results.

The accuracy of opening stress measurements will be the subject of future work conducted at Langley and a round-robin test program sponsored under task group E24.04.04 of ASTM. Other future work at Langley on stress opening measurements will measure crack opening stresses during spectrum loading. In this work, load spectra representative of both transport and fighter aircraft will be used in the testing of aluminum alloy specimens.

In the current understanding of fracture mechanics, K_{eff} appears to be a good parameter for correlating crack growth data. Therefore, accurate measurements of crack opening stresses as well as a thorough understanding of the role of these stresses in the fatigue process is an important part of the damage tolerant design methodology. If fracture mechanics concepts are going to enhance the fatigue design of helicopter components, the study of crack opening stresses must be pursued.

Fatigue Life of a Material With a Machining Scratch

As stated previously, the fatigue life of dynamic parts of helicopters is currently determined by a safe life analysis where stress versus life cycle curves are determined from constant amplitude tests on actual components. Because of the complex configuration of some components, machining scratches can be left on the surface of finished parts. If parts without scratches are used to define S-N curves and failures occur in service as a result of these scratches, the statistical validity of the predicted fatigue life is questionable.

To assess the effect of machining scratches on the fatigue life of 4340 high strength steel, constant amplitude fatigue tests were run on unnotched specimens with and without a 0.05mm (0.002 inch) deep machining scratch. Specimens with scratches that had been shot peened were also tested to see if the compressive residual stresses from the shot peening would provide any relief from the stress concentration caused by the scratch. The magnitude of the residual stresses produced by the shot peening was determined by x-ray diffraction measurements. To assess the effect of shot peening on the fatigue life of materials without machining imperfections, tests were also run on specimens that had been shot peened but contained no scratches.

Figure 8 shows some of the results of these tests where the alternating stress level, S_a , is plotted against fatigue life, N. As can be seen in this

figure the machining scratch caused about a 40% reduction in the material endurance limit. The tests on the specimens that had been shot peened showed that the compressive residual stresses produced by the shot peening almost eliminated the effects of the stress concentration caused by the scratch. For the specimens without machining imperfections that had been shot peened, only about a 10% increase in the endurance limit was noted. The x-ray diffraction measurements of the compressive residual stresses produced by the shot peening ranged from 414 MPa to 621 MPa (60 to 90 ksi). The compressive residual stresses reached a zero stress level at about 0.152 mm (0.006 inches) below the specimen surface.

These tests have shown that a machining scratch significantly reduces the fatigue strength of a high strength steel. However, shot peening was shown to negate the effects of the scratch. Analytically predicting the effects of residual stresses on fatigue life of components is still difficult due mainly to the difficulty in experimentally determining the level of residual stress. The X-ray diffraction technique is showing great promise in improving this situation, but before life predictions that account for residual stresses can be made with a high degree of confidence, joint analytical and experimental programs need to be undertaken that will prove the reliability of the X-ray diffraction measurements.

Ground-Air-Ground Correction Factor for Miner's Rule

In the safe life analysis of aircraft structures, a linear cumulative damage rule like the Miner rule is usually used to predict fatigue life. In spite of the many inadequacies in this type of analysis (ref. 16 to 19), no new theory has replaced the Miner analysis with any significant improvement. Various techniques have been used with the basic concept developed by Miner, in the hope of eliminating some of these inadequacies (ref. 20 to 22). One of the deficiencies of this analysis is its inability to account for sequence effects (load interaction) which are usually present in spectrum loading (ref. 17). In a recent survey of the helicopter industry a hypothetical fatigue life problem was posed that sought the calculation of the fatigue life of a component called the pitch link (ref. 23). In all of the proposed solutions (ref. 24 to 30), the linear cumulative damage theory formed the basis of the life predictions. Both cycle counting and peak value analysis of the flight loads were used to calculate fatigue life. However, because of the significant dissimilarities in methodology in the industry, ground-air-ground (GAG) cycles were not included in the problem.

Current research is being aimed at aiding the safe life designer with a method for including a correction factor in the Miner cumulative damage rule to account for the damage caused by GAG cycles. Simple spectrum block loading similar to that shown in figure 9 will initially be used to assess the upper bounds of the damage caused by these cycles. In an attempt to generalize these correction factors to more realistic load spectra, tests will also be conducted using the standardized helicopter load spectra known as HELIX and FELIX (ref. 7). Previous work has shown that when Miner's rule was used to predict the fatigue life of test coupons tested using the HELIX/FELIX spectra, the fatigue life was overestimated (ref. 31).

Local Strain Method for Predicting Fatigue Life

Over the last two decades a technique has been developed to predict fatigue life using safe-life methodology but concentrating on the area of the structure where maximum damage is actually being accumulated. This technique, called the local strain approach, calculates fatigue life based on the local strains at a notch(ref. 22 and 32). This method takes into account such factors as the mean stress, state of stress, and the effect of local notch plasticity. These factors are still combined into a linear cumulative damage analysis.

Tests are currently being conducted on 4340 steel using the load spectra called HELIX(ref. 7) to simulate the variable cyclic loading usually experienced by dynamic helicopter components. Actual air-to-air combat spectra will also be used as test loads. Test lives will be compared to lives predicted using the local strain approach.

These series of tests are concentrating on using load spectra as opposed to constant amplitude loads since a great weakness in the present design of helicopters is the lack of spectrum tests in the design process. For future work, actual load spectra from various helicopter components must be obtained, since as noted by Dowling(ref. 32), the uncertainties in predictions associated with the choice of a life estimation method may be small compared to the uncertainties which now exist in the definition of helicopter load spectra.

ANALYSIS

Crack Closure Model for Predicting Fatigue Life

As stated previously, the design of most fixed-wing aircraft structures is based on a damage tolerance approach where crack growth analysis is an essential part of the design process. Since about 1970, many crack growth models have been proposed to predict the life of structures. All of these models recognize the need to account for load interaction effects which cause such crack growth phenomena as retardation and acceleration and almost all are based on either crack tip plasticity or crack closure concepts(ref. 33). Two models based on the crack tip plasticity concept are those by Wheeler(ref. 34) and Willenborg(ref. 35). Almost all models based on the plasticity concept use one of these two models as their basis. The Wheeler model accounts for crack growth retardation by employing the concept of yield zone interaction. In this concept, crack growth is retarded if the yield zone of current loads lie within the boundaries of the yield zone of previous high loads. The Wheeler model uses a crack growth retardation parameter that includes an empirically determined constant which is dependent on the material and loading. The Willenborg model accounts for retardation by using the yield zone interaction concepts conceived by Wheeler to determine a so-called "effective" stress that reflects the stress reduction that occurs as a result of overloads. Neither of these models account for the possible counteracting effect on

retardation caused by negative peak loads. A model first developed by Johnson(ref. 36) in 1975 to account for retardation and acceleration, uses Forman's crack growth equation(ref. 37), but uses an "effective" stress ratio which is adjusted for each load cycle to account for load interaction. This model is known as the Multi-Parameter Yield Zone(MPYZ) model.

Crack growth models which account for the concept of the physical crack actually closing before the applied load reaches zero are known as crack closure models. The crack closure phenomena was first noted as a result of the non-linear load displacement behavior of a cracked sheet thus suggesting that the structure has a varying geometry which could only be explained by the crack closing prior to complete unloading(ref. 9). The crack closure crack growth models not only account for retardation and acceleration, but also for delayed retardation. As stated previously in this paper, a crack closure model developed by Newman(ref. 5) has also been used to model the behavior of the so-called "small-crack" effect(ref. 4).

The closure model developed by Newman(ref. 5) at NASA Langley, uses Elber's basic concept of the closure phenomena which states that only that portion of the cyclic load which is above the crack opening load causes the crack to grow. Thus the form of the stress intensity factor that is used to correlate crack growth data is called the effective stress intensity range, ΔK_{eff} , and is essentially calculated by using the difference between the maximum stress in the load cycle and the crack opening stress.

Newman's model uses a modified form of Dugdale's elastic-plastic solution(ref. 38) for stresses and displacements in a cracked body. In Newman's modification of Dugdale's model, plastic deformations at the crack tip are retained in the wake of the crack as it grows. This plastic wake is shown schematically in figure 10, where the shaded regions indicate material that has been plastically deformed. The plastic deformations in the wake cause the crack surfaces to come in contact before the unloading reaches zero. When the load is increased again, the applied stress at which the crack surfaces become fully separated(zero contact stress) is characteristically called the "crack opening stress". For a detailed description of Newman's closure model and how crack growth rates are calculated, see reference 5.

As an illustration of the ability of this model to correlate crack growth data under constant amplitude loading, figure 11 shows crack growth rates for 2219-T851 aluminum alloy at various stress ratios. The solid lines in this figure are a result of calculations using Newman's closure model and the dots are the experimental data points. The predicted crack growth curves are in good agreement with the experimental data. As an example of this model's ability to correlate data from spectrum load tests, figure 12 shows crack-length against load cycle data for a typical fighter spectrum. The specimens were subjected to the same spectrum, but with different load amplification factors(0.2, 0.3, and 0.4) applied to the spectrum loads. Again good agreement is shown between the predicted curves(dashed and solid lines) and the experimental data points when the α factor, which indicates the stress state, is accounted for. For further comparisons between experimental data and closure model predictions, see references 5 and 39.

The crack closure model is an excellent example of the ability of an analytical tool to predict the fatigue life of aircraft structures. As stated previously, this model is currently being used in the investigation of the small-crack effect in 4340 steel, a material often used in the design of helicopter dynamic rotor components.

Boundary-Force Method For Stress Analysis Of Cracked Plates

During the design process, stress analyses are performed to calculate stress concentration factors for holes or notches or stress intensity factors for cracks. Among today's analysis tools, the finite element method (FEM) appears to be the most widely used numerical analysis method. However, recently a new form of an indirect boundary element method (BEM) developed by Tan(ref. 40) at NASA Langley is seeing more widespread use because of its efficiency in modeling the structure which is being analysed. As opposed to the FEM, where usually a relative large number of elements are needed to accurately model the entire structure, in the BEM only the boundaries of the region of interest are modeled.

Two earlier BEMs proposed by Nisitani(ref. 41) and Isida(ref. 42) were called "body force" methods since the unknowns were body force densities in the x- and y- directions and a crack was modeled as a very slender elliptical notch. Tan's Boundary Force Method (BFM) uses Erodogan's analytical solution for concentrated forces and a moment in an infinite plate with a crack(ref. 43), thus, eliminating the need to model the crack. In the BFM, the unknowns are not only the concentrated forces in the x- and y- directions, but also the moments on each segment of the discretized boundaries. The essential differences between Tan's BFM and the other BEM's mentioned are in the fundamental solutions, the treatment of the boundary conditions, and the treatment of the crack faces. For a more detailed account of these differences see reference 40.

To compare the accuracy obtained by satisfying the boundary conditions in terms of resultant forces and moments to that of resultant forces only, a center crack tension specimen was analyzed using the two methods. Figure 13 shows the relative error of these two methods where the relative error is defined as

$$\text{Relative error} = \frac{K_{\text{computed}} - K_{\text{ref}}}{K_{\text{ref}}}$$

where K_{computed} is the stress intensity factor computed by either method and K_{ref} is the reference value taken from the literature. These data show that for the same number of degrees of freedom, Tan's "force and moment" formulation gives a solution which is more accurate. The data in figure 13 shows that Tan's method gives a solution within 1% of the reference solution with as few as 24 degrees of freedom.

Figure 14 shows the BFM solution of the stress-intensity factor for a crack located between four holes. This configuration simulates the effect of a stringer on a propagating crack. This is a rather complex configuration where few stress-intensity solutions are available. The solution shown in figure 14 predicts that the stress intensity will increase until the crack reaches the center-line of the hole at which point it decreases thus simulating the effect of the stringer on the propagating crack and showing the probable retarding of the crack growth and possibly its arrest.

Three-Dimensional Finite-Element Analysis for Cracked and Uncracked Bodies

Prior to the late 1970's, two-dimensional elastic analyses were usually used to calculate stress intensity factors. These analyses approximated the real crack environment being analysed by assuming the two-dimensional states of stress of either plane-stress or plane-strain. Since these states of stress are an engineering approximation of the actual three-dimensional problem, researchers have attempted to solve Navier's equations of equilibrium for the stress field near the crack front. Only a few successful solutions have been developed and these were limited to such crack configurations as the penny-shaped and elliptical crack in an infinite solid(ref. 44). Since the closed-form solutions proved to be very difficult to obtain, several numerical approximations were developed(ref. 45 to 47).

Of these approximate methods, the finite-element method has been the most widely used. However, in most of the finite-element solutions the stress intensity factors were calculated by using the crack-opening displacements and two-dimensional plane-strain assumptions. This approach is again an approximation of the real three-dimensional situation and is justified only near the middle of the specimen thickness where plane-strain conditions may exist. In 1977, Raju and Newman at NASA Langley published a paper on three-dimensional finite-element analysis using a nodal force method to calculate the mode I stress intensity factors along the crack front(ref. 48). This method does not require any prior assumptions of plane-strain or plane-stress. In this paper, Raju and Newman investigated the stress-intensity factor across the thickness for such commonly used fracture specimens as the center-crack tension, single- and double-edge-crack tension, and the compact tension specimen(shown in figure 15). An example of some of the results from this paper is shown in figure 16 for the single-edge-crack tension specimen. The figure shows that the stress-intensity factors are nearly uniform over most of the specimen thickness, but are lower than the plane-strain value near the free surface where the plane-strain assumptions would be questionable. For the rest of the results obtained by Raju and Newman, see reference 48.

In 1979 Raju and Newman continued their work on the analysis of the three-dimensional problem by developing stress-intensity factors for surface cracks(ref. 49). In this work, they modeled shallow and deep semi-elliptical surface cracks in plates subjected to uniform tension. Figure 17 shows the results of a convergence study for a deep semi-elliptic surface

crack. The two finest models give stress-intensity factors within about 1% of each other. In this work they also compared their finite-element results for an embedded elliptical crack with an exact solution developed by Green and Sneddon(ref. 50). In general, Raju and Newman's solution agreed with the exact solution within 1% along most of the crack front.

More recently, Newman and Raju(ref. 51) have presented a paper where stress-intensity-factor equations were developed for several crack configurations from stress-intensity-factors determined from three-dimensional finite-element analysis. Prior to this paper, most of the stress-intensity solutions for cracks have been from approximate analytical solutions where most of the results were for limited ranges of parameters and were presented in the form of curves or tables(ref. 52 to 54). Obviously, an equational form for the stress-intensity factors is preferred because it is easier to use than curves and tables. These equations were developed for tension and bending loads over a wide range of crack configuration parameters such as the ratio of the crack depth to plate thickness(a/t), the ratio of crack depth to crack length(a/c), the ratio of hole radius to plate thickness(r/t), and the effect of plate width, b . The crack configurations considered are shown in figure 18. These include an embedded semi-elliptical crack, a semi-elliptical surface crack, a quarter-elliptical corner crack, a semi-elliptical surface crack at a circular hole, and a quarter-elliptical corner crack at a circular hole in finite thickness plates. An example of the equational form for the embedded semi-elliptical crack is

$$K = S_t(\pi a/Q)^{1/2} F_e(a/c, a/t, c/b, \phi)$$

where S_t is the remotely applied stress, a is the crack depth, and Q is the shape factor for an ellipse and is given by the square of the complete elliptic integral of the second kind. The function F_e accounts for the influence of the crack shape(a/c), crack size(a/t), finite width(c/b), and the angular location(ϕ).

Multigrid Methods In Structural Mechanics

In the finite element method of structural analysis, it is necessary to solve large systems of simultaneous equations. Currently, these equations are usually solved using a direct solution technique such as Gaussian elimination or Cholesky decomposition. These solution techniques are essentially like solving the equation of a straight line, $y=mx+b$. For a structural problem with many degrees of freedom this can involve a large amount of computational time.

Recently, a paper published by Raju et al(ref. 55) at NASA Langley proposed the use of a solution technique called the multigrid method which has been used to solve certain classes of partial differential equations in the field of fluid mechanics(ref. 56 and 57). This method is an iterative technique which assumes an initial answer for the unknown nodal

displacements and iterates through an algorithm until the current estimate of the unknowns are within a predetermined tolerance (or error).

One of the main purposes in Raju's paper was to gain an understanding of the multigrid method for use in structural mechanics applications. Hence, in this paper the multigrid technique was applied to the finite element analysis of the deflections of a simply supported Bernoulli-Euler beam(ref. 55).

This work on the simply supported beam has laid the foundation for extending this work to two- and three-dimensional problems and to include problems in structural analysis where singularities exist such as those at the tip of a crack. The final goal is a black box algebraic multigrid solution package for finite element analysis that could be 10 times faster than the direct solution techniques currently used in finite element analysis.

J-Integral Resistance Curve for Ductile Materials

The stress intensity factor range, ΔK , which has been used effectively to correlate crack growth data in metal structures is generally limited to use in situations that can be described as small-scale yielding at the crack tip. This will be the case for most aircraft structures. However, in a situation where large amounts of plastic deformation occur a parameter called the J-integral is often used to correlate crack growth and fracture data(ref. 58 and 59). The J-integral is defined as the rate of change of the total potential energy of the specimen with respect to the crack length(ref. 60). In contrast to K, the J-integral depends on the amount of crack growth.

Currently, the test procedures for determining J-R curves (crack-growth resistance curves based on the J-integral) show a dependency on specimen type(ref. 61). Two specimens which are often used in determining J-R curves are the three-point bend specimen and the compact specimen, shown in figure 19. Because of the J-R curves dependency on specimen type a task group from ASTM Committee E24 was initiated to develop a test procedure that would give J-R curves that were not dependent on specimen configuration(ref. 62).

In 1980, a round robin test program was conducted in 19 laboratories to measure J-R curves on HY-130 steel plate to evaluate the tentative test procedure developed by the ASTM task group. Figure 20 shows curves from one of these laboratories for both the compact and the bend specimen. The lack of uniqueness shown by these data showed the need for further investigations.

Recent work at NASA Langley was initiated to analyze numerically the discrepancy between the compact and bend specimen J-R curves. The approach taken was to model the fracture process in the two specimens using a two-dimensional, elastic-plastic, finite-element computer program(ref. 63) with a critical crack-tip-opening displacement failure criterion(ref. 64). The results from the analysis are shown in figure 21. As seen in this figure,

up to the maximum load, the J curves calculated from this analysis agreed well for both specimen configurations.

CONCLUDING REMARKS

Most dynamic components in helicopters are designed with a safe-life, constant amplitude testing approach that has not changed in many years. In contrast, the fatigue methodology in other industries has advanced significantly in the last two decades. In this paper a review is presented of the current research at the NASA Langley Research Center and U.S. Army Aerostructures Directorate at Langley which might aid the helicopter industry in enhancing the fatigue and fracture design methodology for metallic components.

In the area of testing, Langley research has shown that "small" cracks do grow at stress intensity ranges below the so-called large crack threshold. Crack opening stress measurements have shown that when the stress intensity range is calculated using only the stress range above the crack opening stress, a good correlation of crack growth data is obtained. Further work has shown that a machining scratch (0.05 mm deep) can reduce the fatigue life of a high strength steel by 40%, but shot peening can almost eliminate the effects of the stress concentration caused by a scratch.

In the area of analysis, a crack closure model for predicting fatigue life has been developed and used to predict fatigue life for both constant-amplitude and spectrum loading. Since the ability of the crack closure model to predict fatigue life is dependent upon an accurate stress analysis, a three-dimensional finite element program has been developed to calculate the stress intensity factors needed in the closure model. A boundary force method for calculating stress intensity factors has also been developed. This method is more efficient in modeling the structure being analysed than the finite element method, since only the boundary of the structure needs to be modeled.

REFERENCES

1. Pearson, S.: "Initiation of Fatigue Cracks in Commercial Aluminum Alloys and the Subsequent Propagation of Very Short Cracks," Engineering Fracture Mechanics, Vol. 7, No. 2, 1975, pp. 235-247.
2. Ritchie, R. O. and Lankford, J.: "Overview of the Small Crack Problem", Proceedings of the Second Engineering Foundation International Conference/Workshop on Small Fatigue Cracks, 1986, pp. 1-5.

3. Nisitai, H.: "Behavior of Small Cracks in Fatigue and Relating Phenomena," Current Research on Fatigue Cracks, The Society of Materials Science, Japan, pp. 1-22.
4. Newman, J. C., Jr.; Swain, M. H.; and Phillips, E. P.: "An Assessment of the Small-Crack Effect for 2024-T3 Aluminum Alloy," Proceedings of the Second Engineering Foundation International Conference/Workshop on "Small Fatigue Cracks", 1986, pp. 427-452.
5. Newman, J. C., Jr.: "A Crack-Closure Model for Predicting Fatigue Crack Growth Under Aircraft Spectrum Loading," Methods and Models for Predicting Fatigue Crack Growth Under Random Loading, ASTM STP 748, eds. J.B. Chang and C.M. Hudson, 1981, pp. 53-84.
6. van Dijk, G. M. and de Jonge, J. B.: "Introduction to a Fighter Aircraft Loading Standard for Fatigue Evaluation FALSTAFF," NLR MP 75017U, May 1975.
7. Edwards, P. R. and Darts, J.: "Standardised Fatigue Loading Sequences for Helicopter Rotors (HELIX and FELIX) Part 1: Background and Fatigue Evaluation," Royal Aircraft Establishment, TR 84084, 1984.
8. Rice, J. R.: in Fatigue Crack Propagation, ASTM STP 415, 1967, p. 247.
9. Elber, W.: "Fatigue Crack Propagation," Ph.D. thesis, University of South Wales, Australia, 1968.
10. Elber, W.: "Fatigue Crack Closure Under Cyclic Tension," Engineering Fracture Mechanics, Vol. 2, No. 1, 1970, pp. 37-45.
11. Schijve, J.: "Fatigue Crack Closure, Observations and Technical Significance," keynote paper at the ASTM International Symposium on Fatigue Crack Closure, Charleston, S.C., May 1986.
12. Phillips, E.P.: "The Influence of Crack Closure on Fatigue Crack Growth Thresholds in 2024-T3 Aluminum Alloy," presented at the ASTM International Symposium on Fatigue Crack Closure in Charleston, S.C., May 1986.
13. Liaw, P.K.; Leax, T.R.; Swaminathan, V.P.; and Donald, J.K.: "Influence of Load Ratio on Near-Threshold Fatigue Crack Propagation Behavior," Scripta Metallurgica, Vol. 16, 1982, pp. 871-876.
14. Ohta, A.; Kosuge, M.; and Sasaki, E.: "Fatigue Crack Closure Over the Range of Stress Ratios from -1 to 0.8 Down to Stress Intensity Threshold Level in HT80 Steel and SUS304 Stainless Steel," International Journal of Fracture, Vol. 14, No. 3, June 1978, pp. 251-264.
15. Elber, W.: "Crack-Closure and Crack-Growth Measurements in Surface-Flawed Titanium Alloy Ti-6Al-4V", NASA TN D-8010, National Aeronautics and Space Administration, Washington, D.C., Sept. 1975.

16. Jacoby, G.: "Comparison of Fatigue Life Estimation Processes for Irregularly Varying Loads," Proceedings of the Third Conference on Dimensioning, Budapest, 1968.
17. Gassner, E. and Lipp W.: "Long Life Random Fatigue Behavior of Notched Specimens in Service, in Service Duplication Tests, and in Program Tests," ASTM STP 671, Nov. 1977.
18. Shutz, W.: "The Prediction of Fatigue Life in the Crack Initiation and Propagation Stages - A State of the Art Survey," Engineering Fracture Mechanics, Vol. 11, No. 2, 1979.
19. Ryan, J.P.; Berens, A.P.; Coy, R.G.; and Roth, G.J.: "Helicopter Fatigue Load and Life Determination Methods," U.S. Army Air Mobility Research and Development Laboratory, Ft. Eustis, Va., USAAMRDL-TR-75-27, 1975.
20. Haibach, E.: "Fatigue Life Prediction By Amplitude Transformation," Fracture 1977, Vol. 2, ICF4.
21. Buch, A.: "Improvement of Fatigue Life Prediction Accuracy for Various Loading Spectra By Use of Correction Factors," Technion Israel Institute of Technology, TAE No. 581, Nov. 1985.
22. Dowling, N.E.: "A Discussion of Methods for Estimating Fatigue Life," proceedings of SAE Fatigue Conference, Fatigue Conference and Exposition, April 1982.
23. Arden, R.W.: "Hypothetical Fatigue Life Problem," American Helicopter Society Specialists Meeting on Helicopter Fatigue Methodology sponsored by the Midwest Region, preprint no. 18, 1980.
24. Stievenard, G.: "Hypothetical Fatigue Life Problem Application of Aerospatiale Method," American Helicopter Society Specialists Meeting on Helicopter Fatigue Methodology sponsored by the Midwest Region, preprint no. 19, 1980.
25. Aldinio, G. and Alli, A.: "The Agusta's Solution of AHS'S Hypothetical Fatigue Life Problem," American Helicopter Society Specialists Meeting on Helicopter Fatigue Methodology sponsored by the Midwest Region, preprint no. 20, 1980.
26. McCloud, G.W.: "A Method of Determining Safe Service Life for Helicopter Components," American Helicopter Society Specialists Meeting on Helicopter Fatigue Methodology sponsored by the Midwest Region, preprint no. 21, 1980.
27. Thompson, G.H.: "Boeing Vertol Fatigue Life Methodology," American Helicopter Society Specialists Meeting on Helicopter Fatigue Methodology sponsored by the Midwest Region, preprint no. 22, 1980.
28. McDermott, J.: "Hughes Helicopters-Fatigue Life Methodology," American Helicopter Society Specialists Meeting on Helicopter Fatigue Methodology sponsored by the Midwest Region, preprint no. 23, 1980.

29. Hardensen, L.P.: "Fatigue Life Prediction of Helicopter Pitch Link Using Kaman Life Calculation Methods," American Helicopter Society Specialists Meeting on Helicopter Fatigue Methodolgy sponsored by the Midwest Region, preprint no. 24, 1980.
30. Altman, B. and Pratt, J.: "The Challenge of Standardizing Fatigue Methodology," American Helicopter Society Specialists Meeting on Helicopter Fatigue Methodology sponsored by the Midwest Region, preprint no. 25, 1980.
31. Edwards, P.R.: "A Description of Helix and Felix, Standard Fatigue Loading Sequence for Helicopters, and of Related Fatigue Tests Used to Assess Them," Ninth European Rotorcraft Forum, Stresa Italy, 1983.
32. Dowling, N.E.: "Fatigue Failure Predictions for Complicated Stress-Strain Histories," Journal of Materials, Vol. 7, No.1, 1972, pp. 71-87.
33. Ewalds, H.L. and Wanhill, R.J.H.: Fracture Mechanics, Edward Arnold and Delftse Uitgevers Maatschappij Ltd, The Netherlands, 1984.
34. Wheeler, O.E.: Journal of Basic Engineering, Transactions of American Society of Mechanical Engineers, Series D, Vol. 94, No.1, 1972, p. 181.
35. Willenborg, J.D.; Engle, R.M., Jr.; and Wood, H.A.: "A Crack Growth Retardation Model Using Effective Stress Concept," AFFDL-TM-71-1-FBR, Jan. 1971.
36. Johnson, W.S.: "CGR, An Improved Computerized Model to Predict Fatigue Crack Growth Under Spectrum Loading, NSRDC Report 4577, Jan. 1975.
37. Foreman, R.G.; Kearney, V.E.; and Engle, R.M.: Journal of Basic Engineering, Transactions of American Society of Mechanical Engineers, Series D, Vol. 89, No. 3, Sept. 1967, pp. 459-464.
38. Dugdale, D.S.: "Yielding of Steel Sheets Containing Slits," Journal of the Mechanics of the Physics of Solids, Vol. 8, 1960.
39. Newman, J.C., Jr.: "Prediction of Fatigue Crack Growth under Variable-Amplitude and Spectrum Loading Using a Closure Model," ASTM STP 761, 1982, pp. 255-277.
40. Tan, P.W.; Raju, I.S.; and Newman, J.C., Jr.: "Boundary Force Method for Analyzing Two-Dimensional Cracked Bodies," NASA TM-87725, May 1986.
41. Nisitani, H.: "Two-Dimensional Problems Solved Using A Digital Computer," Journal of Jap. Soc. Mech. Engrs., Vol. 70, No. 580, 1967, pp. 627-635.
42. Isida, M.: "A New Procedure of the Body Force Method with Applications to Fracture Mechanics," Numerical Methods in Fracture Mechanics; Proceedings of the First International Conferences, Swansea, Wales, Jan. 1978, pp. 81-94.

43. Erodogan, F.: "On the Stress Distribution in a Plate with Collinear Cuts Under Arbitrary Loads," Proceedings of the Fourth U.S. National Congress of Applied Mechanics, 1962, pp. 547-553.
44. Kassir, M.K. and Sih, G.C.: "Three Dimensional Stress Distribution Around an Elliptical Crack Under Arbitrary Loadings," Trans. ASME, Ser. E, Journal of Applied Mechanics, Vol. 33, No. 3, Sept. 1966, pp. 601-611.
45. Cruse, T.A. and Vanburen, W.: "Three-Dimensional Elastic Analysis of a Fracture Specimen With an Edge Crack," International Journal of Fracture Mechanics, Vol. 7, No. 1, March 1971, pp. 1-15.
46. Tracey, D.M.: "Finite Elements for Three-Dimensional Elastic Crack Analysis," Nuclear Engineering and Design, Vol. 26, No. 2, 1974, pp. 282-290.
47. Atluri, S. and Kathiresan, K.: "An Assumed Displacement Hybrid Finite Element Model for Three-Dimensional Linear-Fracture-Mechanics Analysis," proceedings off the 12th Annual Meeting of the Society of Engineering Science, 1975, pp. 391-399.
48. Raju, I.S. and Newman, J.C., Jr.: "Three-Dimensional Finite-Element Analysis of Finite-Thickness Fracture Specimens," NASA TN D-8414, 1977.
49. Raju, I.S. and Newman, J.C., Jr.: "Stress-Intensity Factors for a Wide Range of Semi-Elliptical Surface Cracks in Finite-Thickness Plates," Engineering Fracture Mechanics, Vol. 11, No. 4, 1979, pp. 817-829.
50. Green, S.E. and Sneddon, I.N.: "The distribution of Stress in the Neighborhood of a Flat Elliptical Crack in an Elastic Solid," proceedings of Cambridge Phil. Soc. 46, 1959.
51. Newman, J.C., Jr. and Raju I.S.: "Stress-Intensity Factor Equations for Cracks in Three-Dimensional Finite Bodies Subjected to Tension and Bending Loads," Computation Methods in the Mechanics of Fracture, Vol. 2 in Computational Methods in Mechanics, (ed.) Atluri, S.N., 1986.
52. Smith, F.W.; Emery, A.F.; and Kobayashi, A.S.: "Stress Intensity Factors for Semi-Circular Cracks, Part 2-Semi-Infinite Solid," Journal of Applied Mechanics 34, No.4, Trans. ASME, Vol. 89, Series E, 1967, pp. 953-959.
53. Heliot, J.; Labbens, R.; and Pellissier-Tanon, A.: "Benchmark Problem No. 1 - Semi-Elliptical Surface Crack," Int. Journal of Frcture 15, 1979, R197-R202.
54. Nishioka, T. and Atluri, S.N.: "Analytical Solution for Embedded Elliptical Cracks, and Finite Element-Alternating Method for Elliptical Surface Cracks, Subjected to Arbitrary Loadings," Engineering Fracture Mechanics, 17 1983, pp.247-268.
55. Raju, I.S.; Bigelow, C.A.; Ta'asan, A.; and Hussaini, M.Y.: "Multigrid Methods in Structural Mechanics," NASA TM-87761, July 1986.

56. Brandt, A.: "Multigrid Techniques: 1984 Guide with Applications to Fluid Dynamics," Monograph, Available as GMD-Studie No. 85 form GMD-F1T, Postfach 1240, D-5205, St. Augustin 1, W. Germany.
57. Jameson, A.: "Solution of the Euler Equations for Two Dimensional Transonic Flow by a Multigrid Method," Applied Math. and Comp., Vol. 13, 1983, pp.327-355.
58. Irwin, G.R.: "Fracture", Encyclopedia of Physics, S. Flugge (ed.), Vol. 6, Springer, Berlin, 1958, pp. 551-590.
59. Rice, J.R.: "A Path Independent Integral and the Aproximate Analysis of Strain Concentrations by Notches and Cracks," Journal of Applied Mechanics, Transactions of ASME, Vol. 90, Series E, No. 2, 1968, pp. 379-386.
60. Broek, D.: Elementary Engineering Fracture Mechanics, Martinus Nijhoff Publishers, The Hague, 1983.
61. Newman, J.C., Jr.; Booth, B.C.; and Shivakumar, K.N.; "An Elastic-Plastic Finite-Element Analysis of the J-Resistance Curve Using A CTOD Criterion," presented at the Eighteenth National Symposium on Fracture Mechanics, Univ. of Colorado, 1985.
62. Albrecht, P.; Andrews, W.R.; Gudas, J.P.; Joyce, J.A.; Loss, F.J.; McCage, D.E.; Schmidt, D.W.; and VanDerSlugs, W.A.; "Tentative Test Procedure for Determining the Plane Strain J(I)-R Curve," Journal of Testing and Evaluation, JTEVA, Vol. 10, No. 6, Nov. 1982, pp. 252-262.
63. Newman, J.C., Jr.: "Finite-Element Analysis of Fatigue Crack Propagation - Including the Effects of Crack Closure," Ph.D. Thesis, Virginia Polytechnic Institute and State University, May 1974.
64. Newman, J.C., Jr.: "Finite-Element Analysis of Initiation, Stable Crack Growth, and Instability Using a Crack-Tip-Opening Displacement Criterion," NASA TM-84564, Oct. 1982.

CRACK-GROWTH RATES FOR SMALL CRACKS

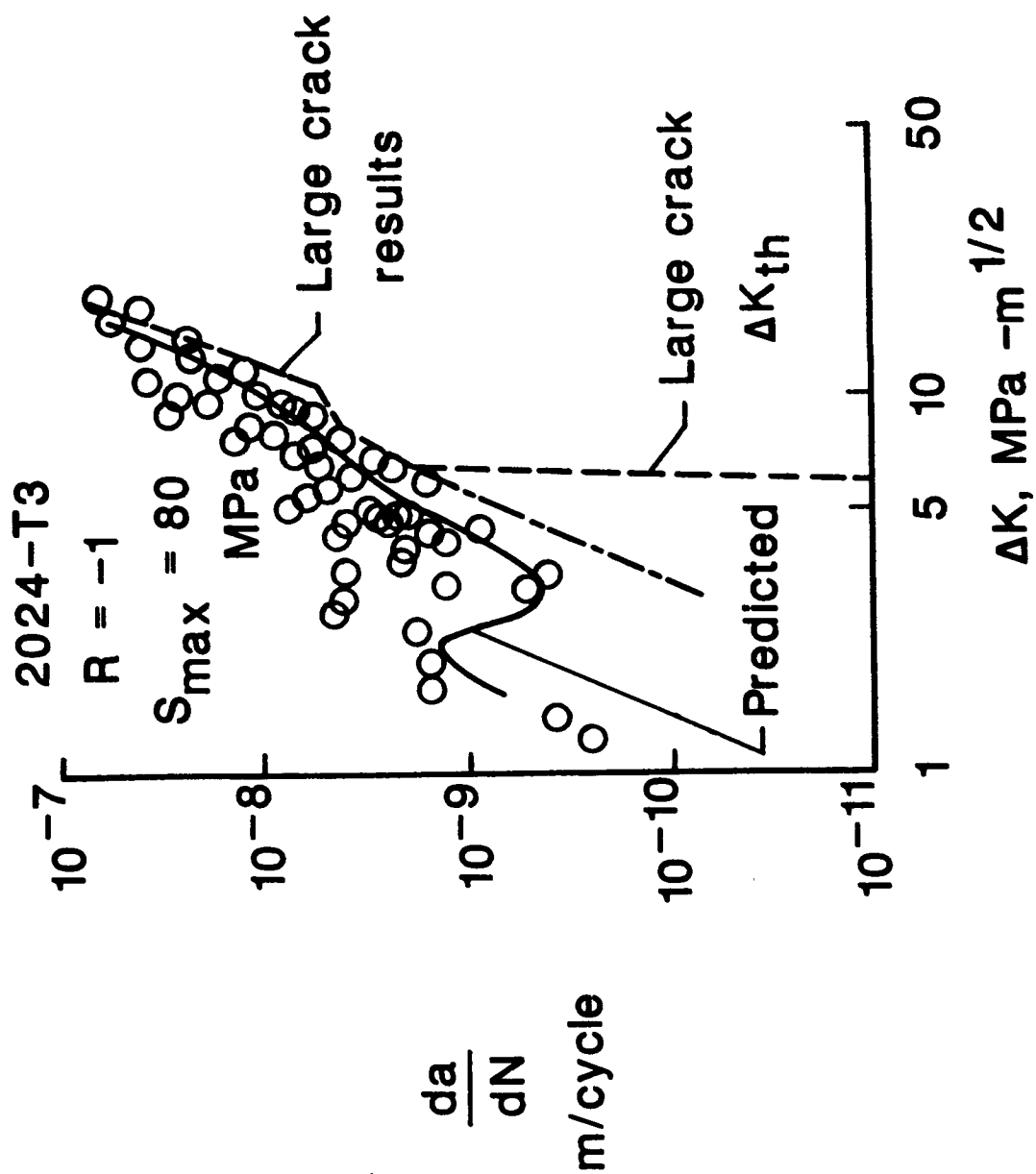


Figure 1.

LIFE-TO-FAILURE DATA FOR NOTCHED SPECIMENS

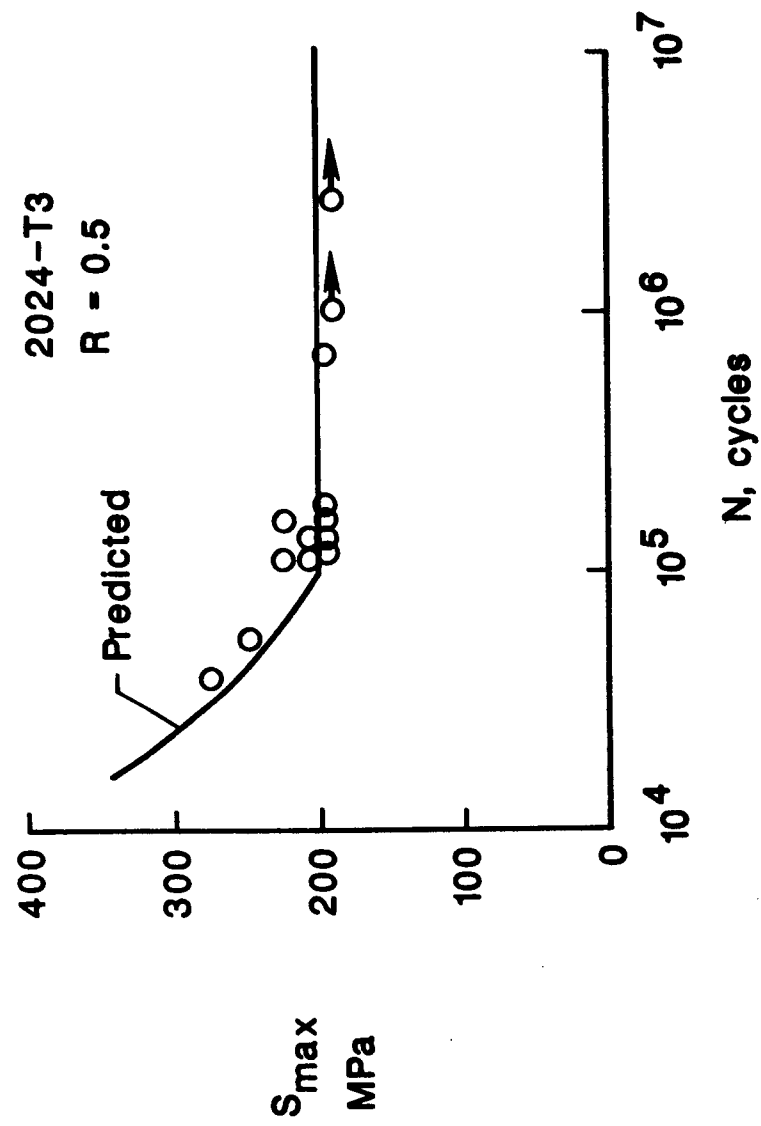


Figure 2.

LIFE-TO-FAILURE DATA FOR A FIGHTER SPECTRUM

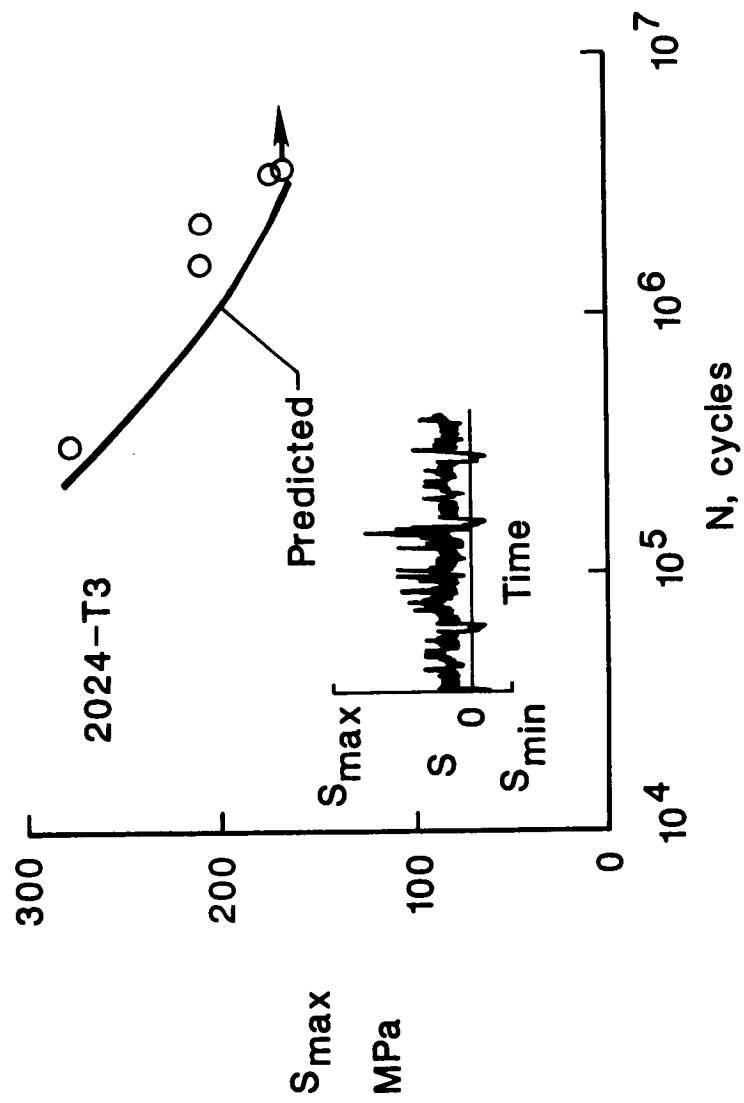


Figure 3.

CRACK GROWTH RATES AT SEVERAL STRESS RATIOS **6% LOAD REDUCTION**

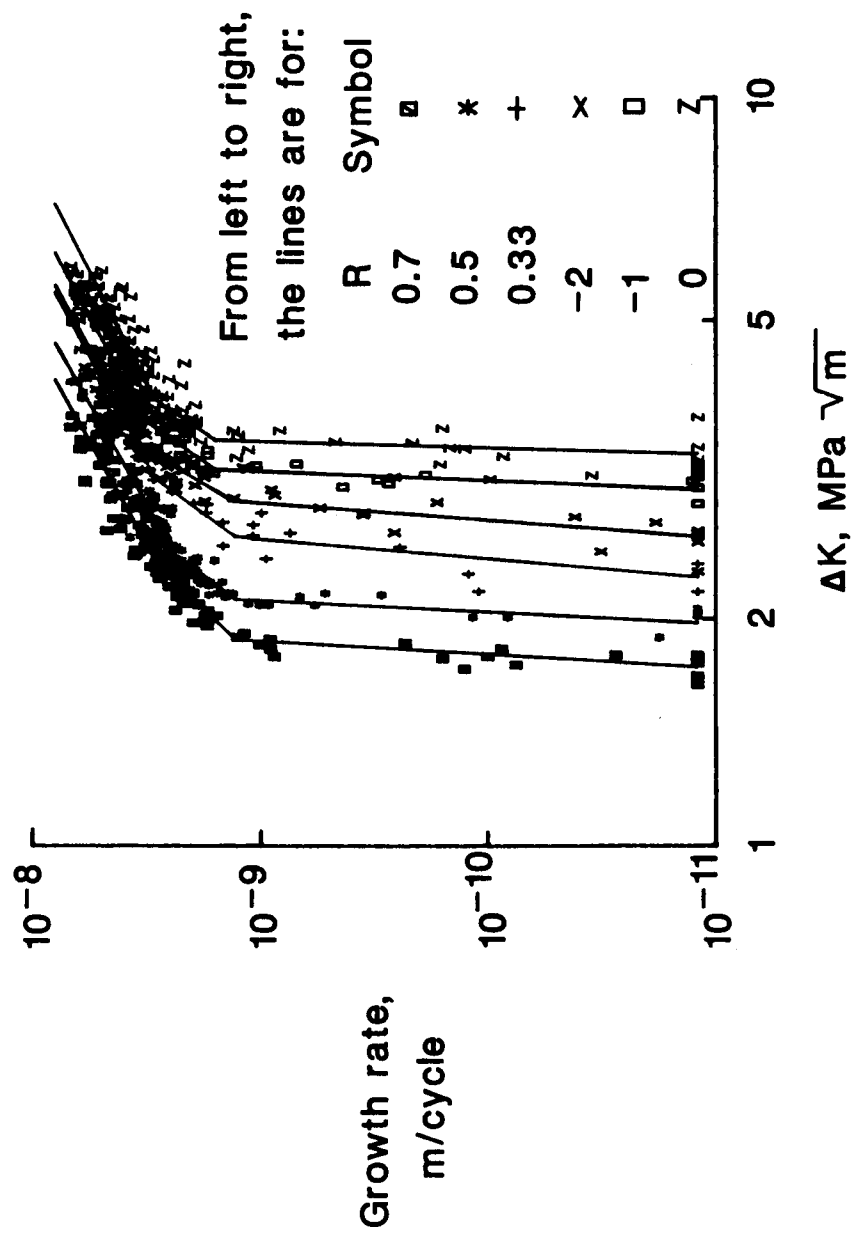


Figure 4.

CRACK OPENING LOADS AT SEVERAL STRESS RATIOS

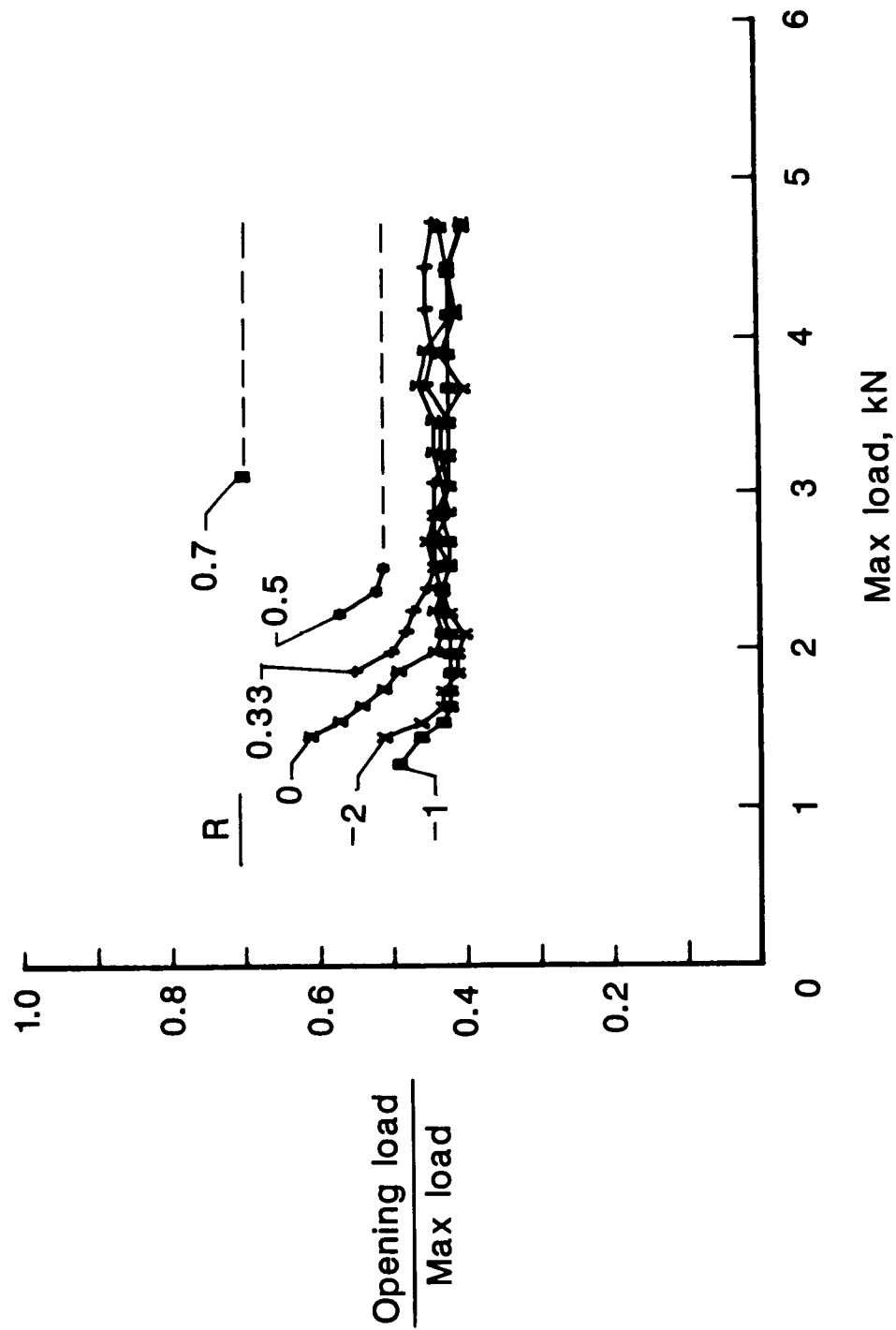


Figure 5.

CRACK GROWTH RATES AT SEVERAL STRESS RATIOS USING ΔK_{eff}

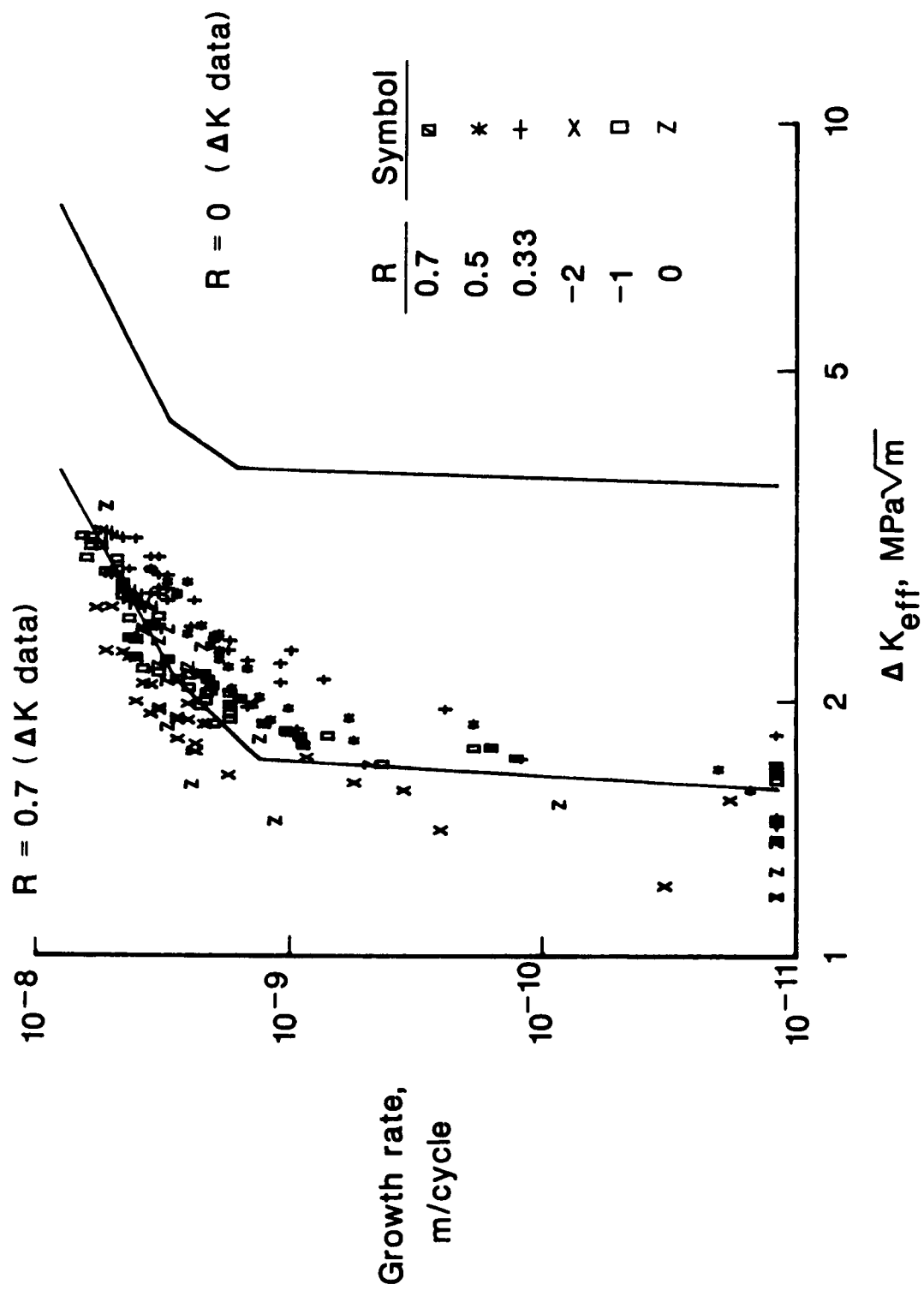


Figure 6.

THRESHOLD ΔK AND ΔK_{eff} VALUES WITH STRESS RATIO

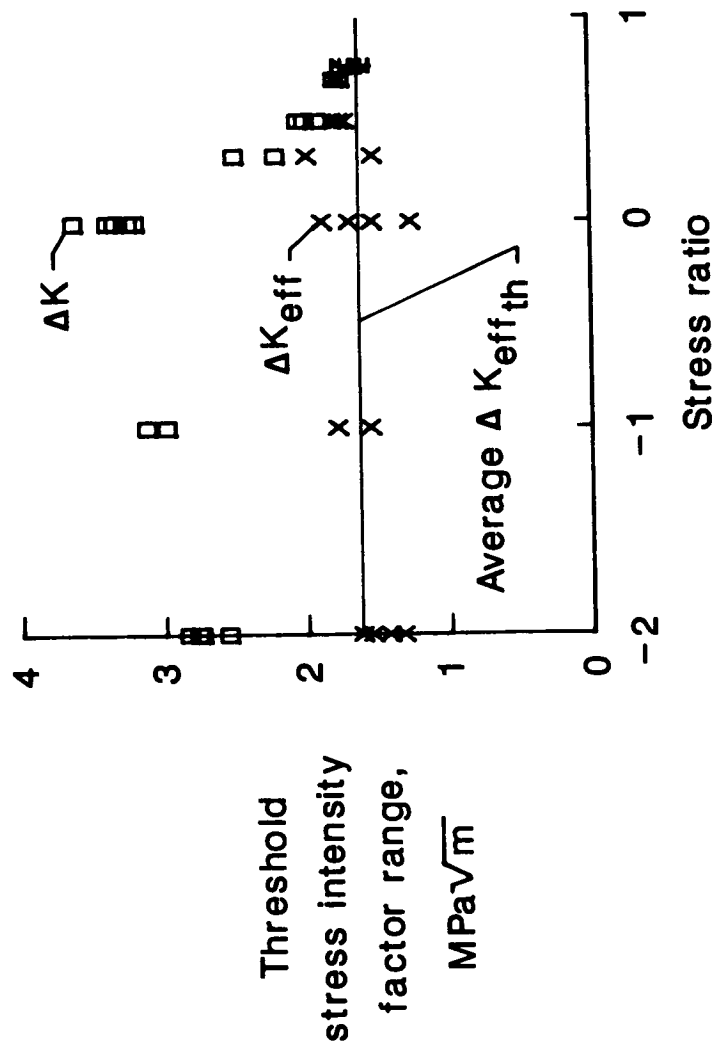


Figure 7.

EFFECT OF MACHINING SCRATCH ON LIFE-CYCLES-TO FAILURE 4340 STEEL

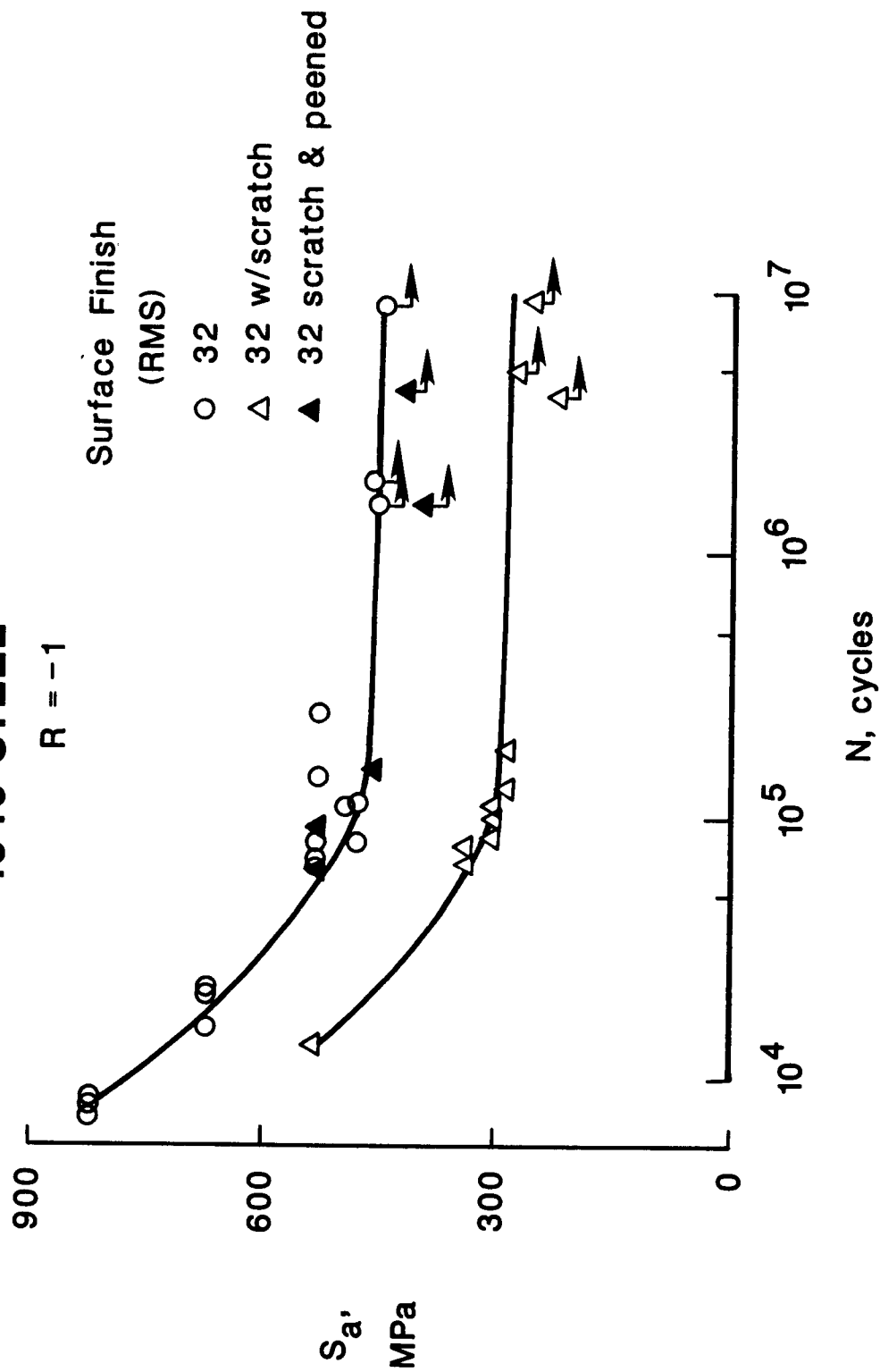


Figure 8.

GROUND-AIR-GROUND (GAG) CYCLES IN BLOCK LOADING

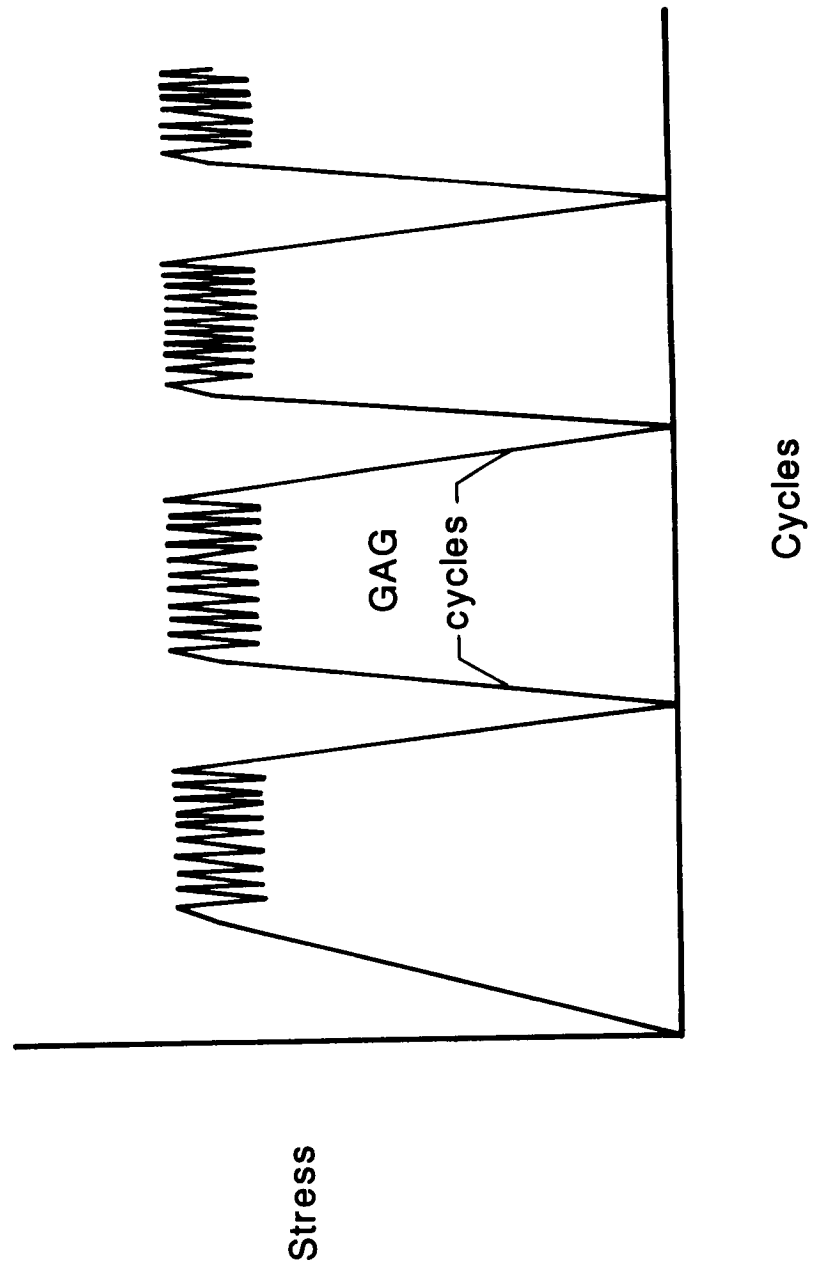


Figure 9.

PLASTIC WAKE IN NEWMAN'S CRACK-CLOSURE MODEL

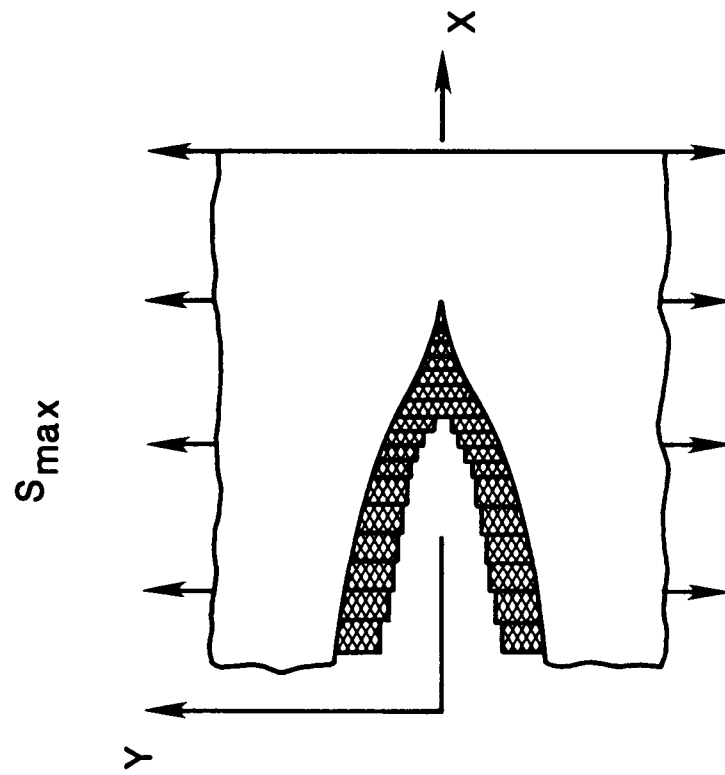


Figure 10.

CLOSURE MODEL PREDICTION OF CRACK GROWTH TESTS

CONSTANT AMPLITUDE TESTS

2219-T851

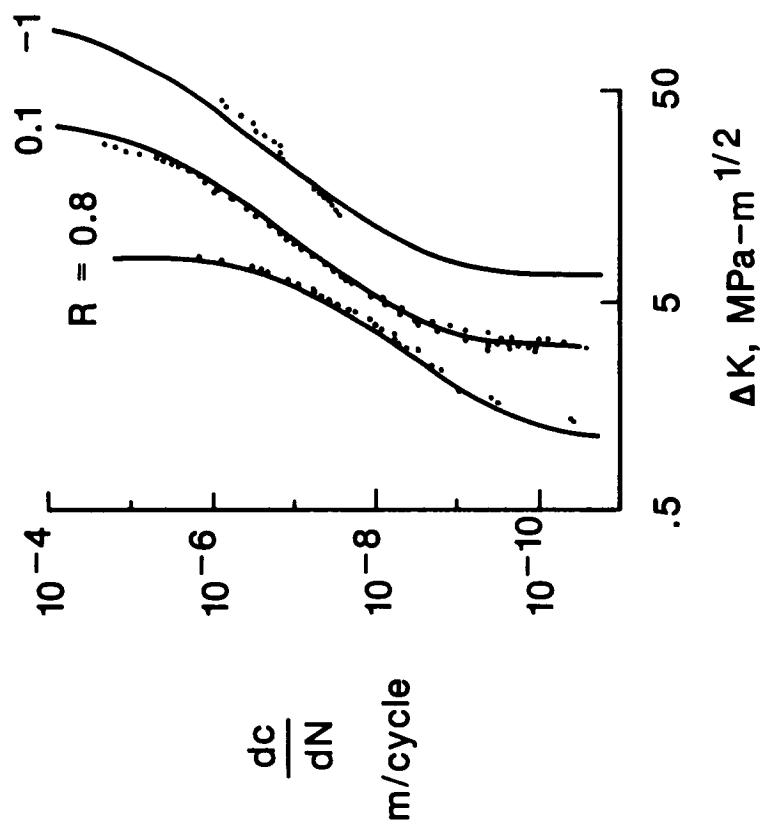


Figure 11.

CLOSURE MODEL PREDICTION OF SPECTRUM LOADING TESTS

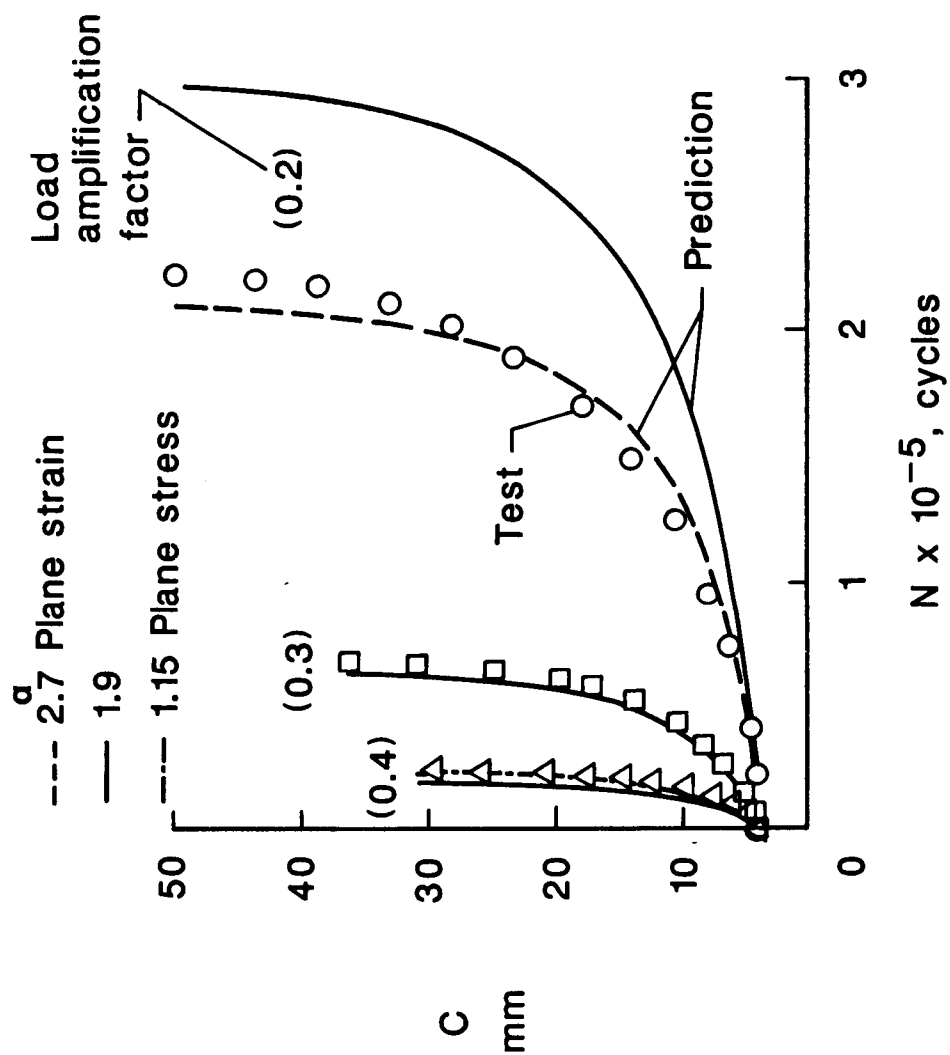


Figure 12.

RELATIVE ERROR IN K FROM TWO BOUNDARY ELEMENT METHODS

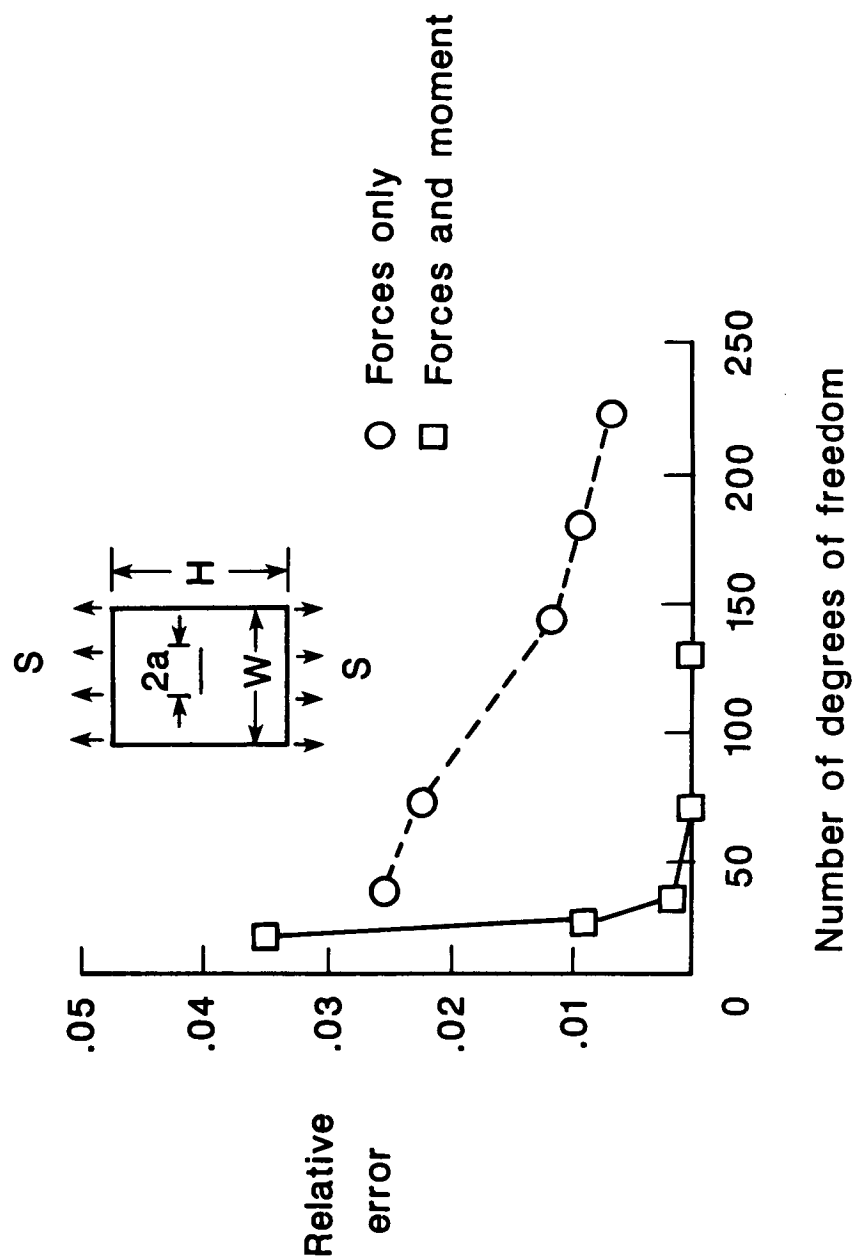


Figure 13.

STRESS INTENSITY FACTOR FROM THE BOUNDARY FORCE METHOD

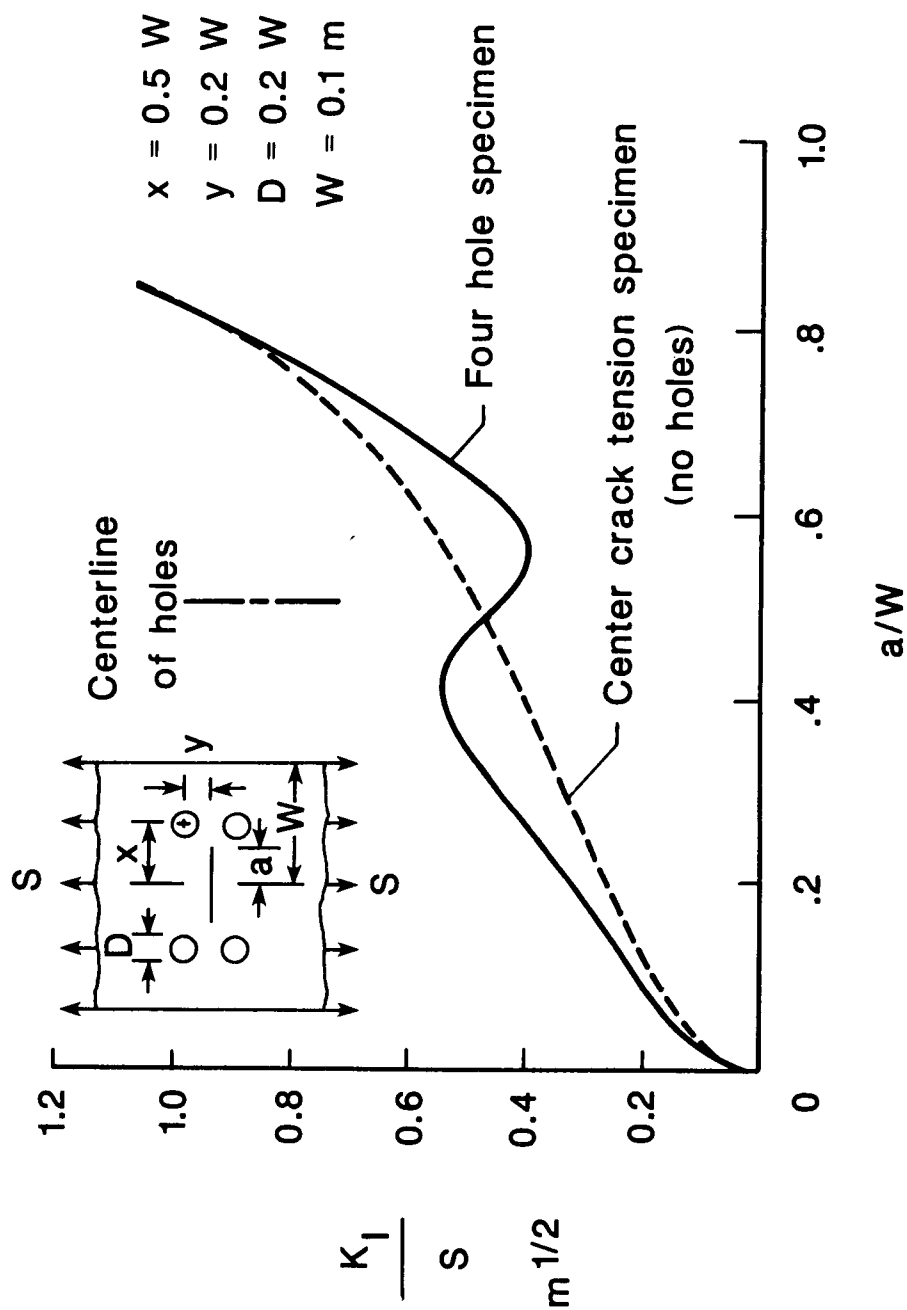
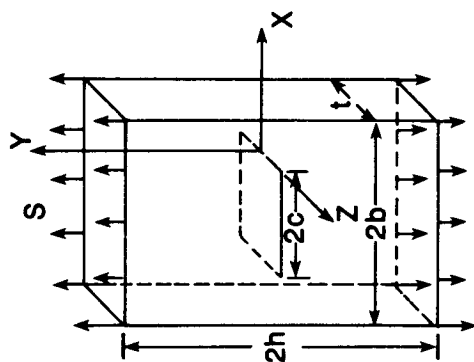
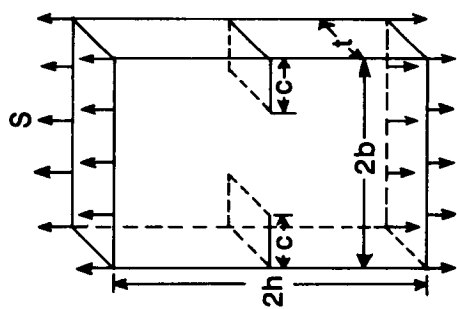


Figure 14.

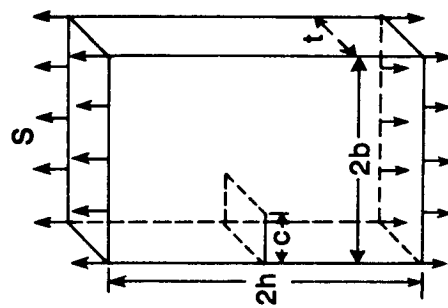
THREE-DIMENSIONAL FRACTURE SPECIMENS



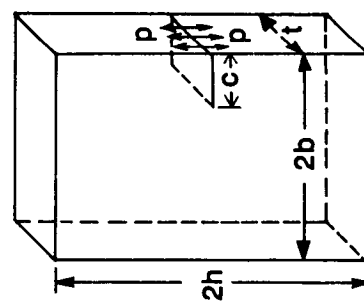
Center crack tension



Double-edge-crack tension



Single-edge-crack tension



Compact

Figure 15.

STRESS-INTENSITY FACTORS FROM 3-D ANALYSIS

SINGLE-EDGE-CRACK-TENSION SPECIMEN

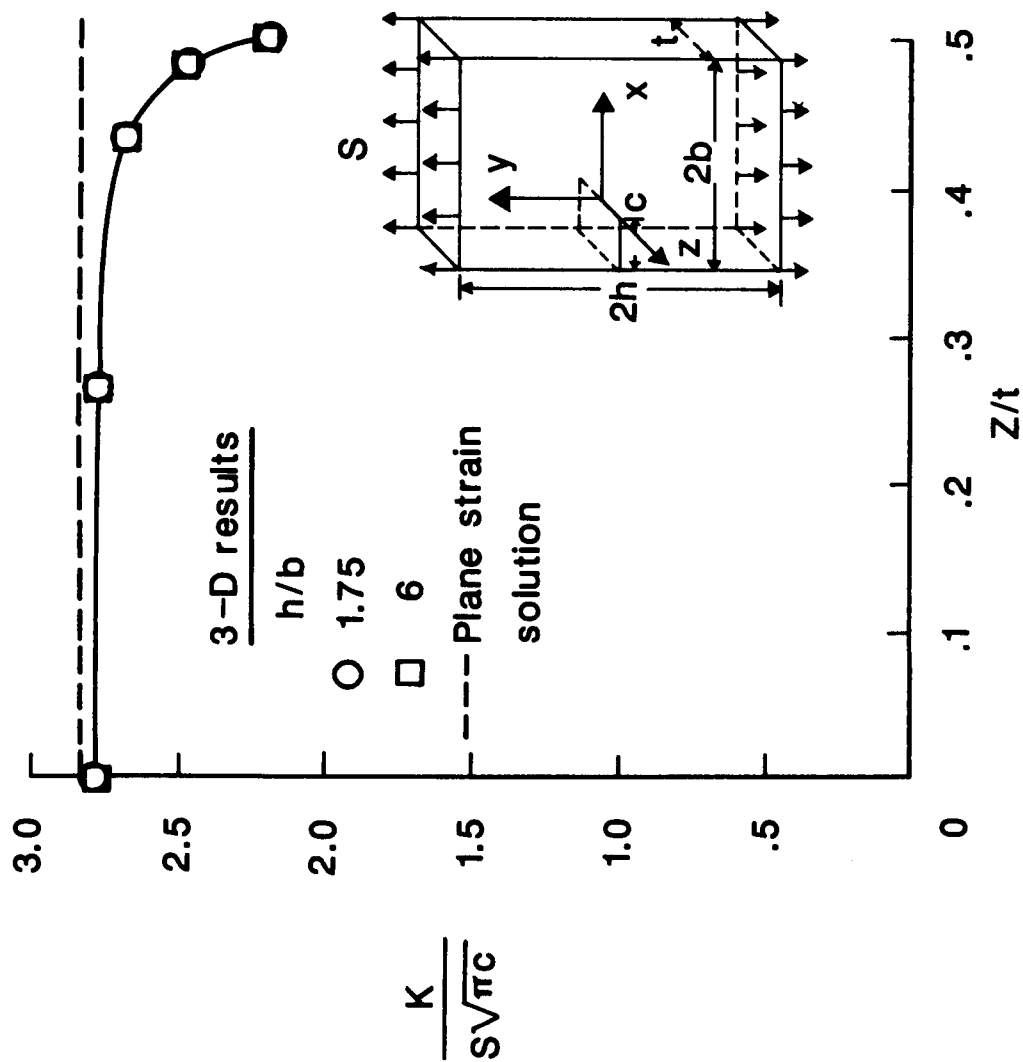


Figure 16.

CONVERGENCE STUDY FOR 3-D STRESS-INTENSITY FACTORS DEEP SEMI-ELLIPTICAL SURFACE CRACK

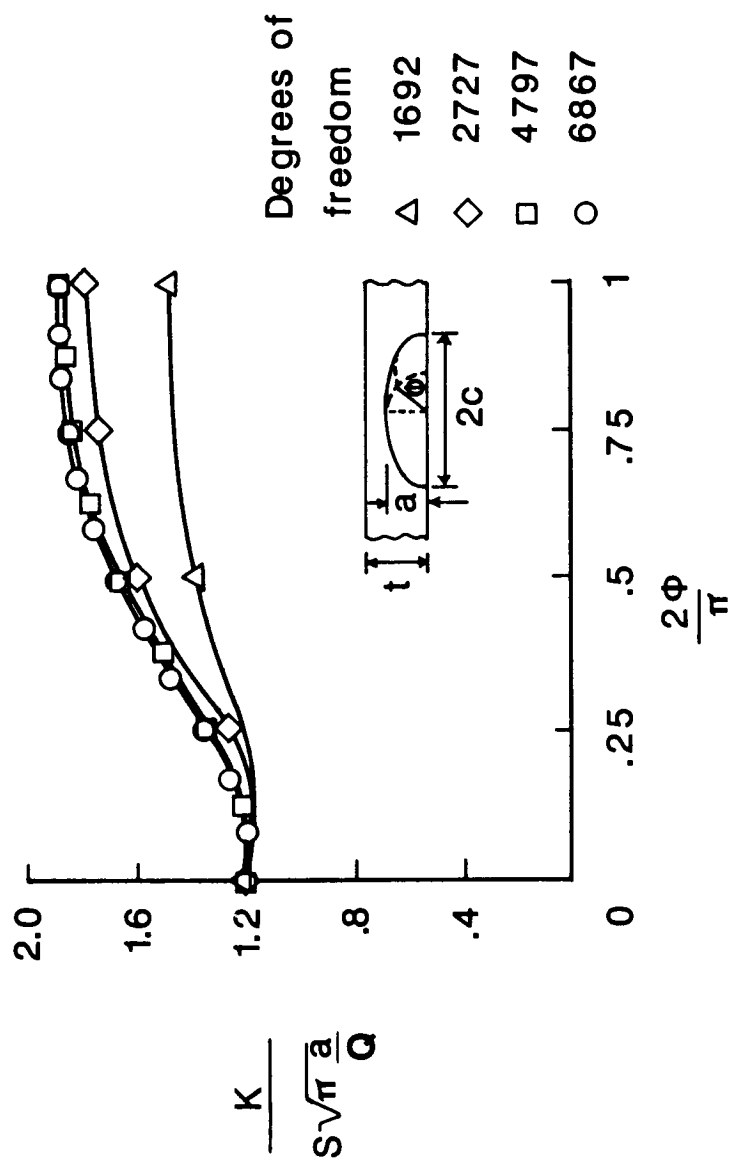


Figure 17.

CRACK CONFIGURATIONS FOR THREE DIMENSIONAL K SOLUTIONS

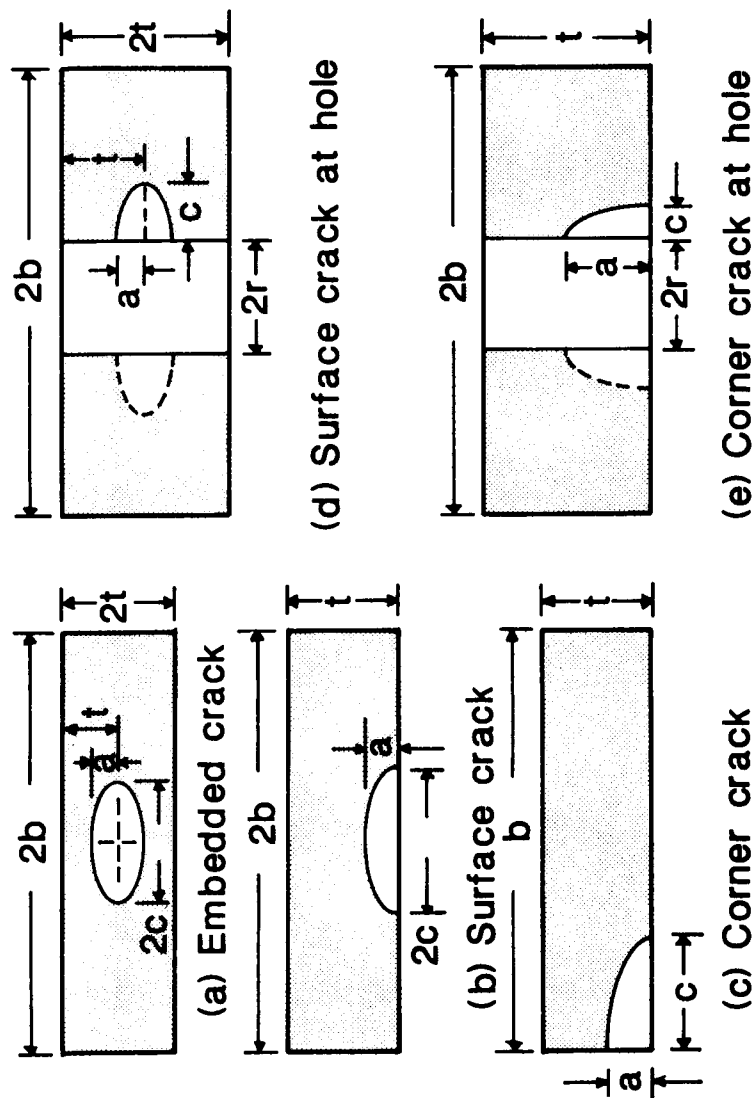
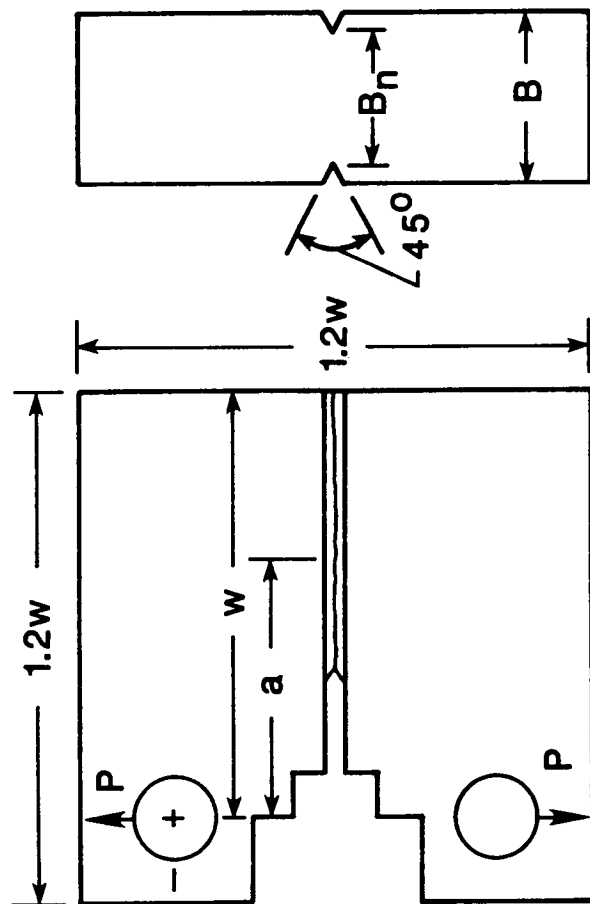
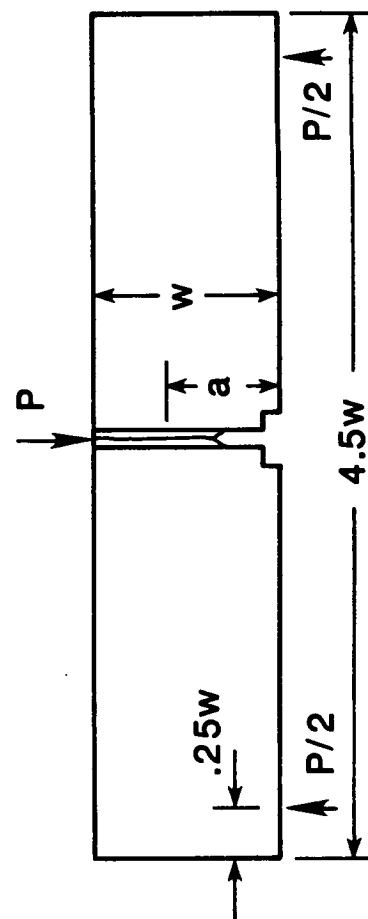


Figure 18.

SPECIMENS FOR DETERMINING J-INTEGRAL RESISTANCE CURVES



(a) J-compact specimen



(b) Bend specimen

Figure 19.

J-INTEGRAL RESISTANCE DATA

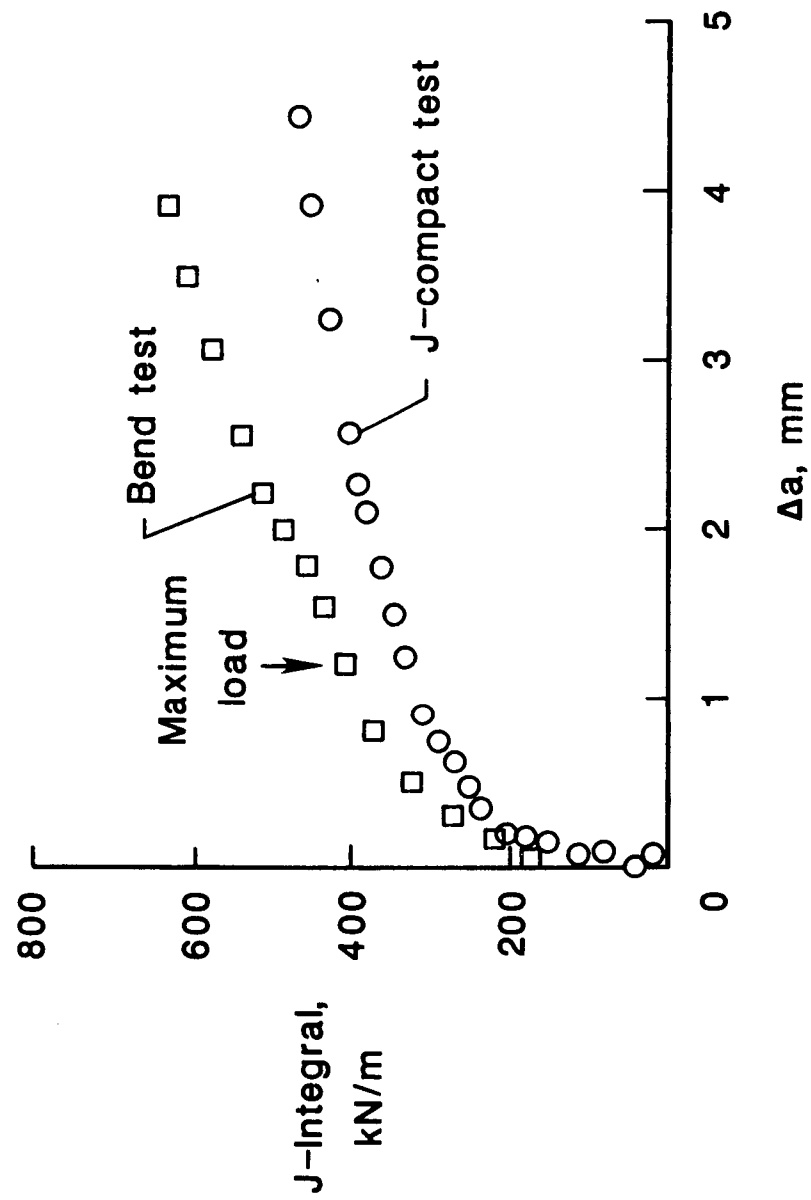


Figure 20.

COMPUTED J-INTEGRAL RESISTANCE CURVES

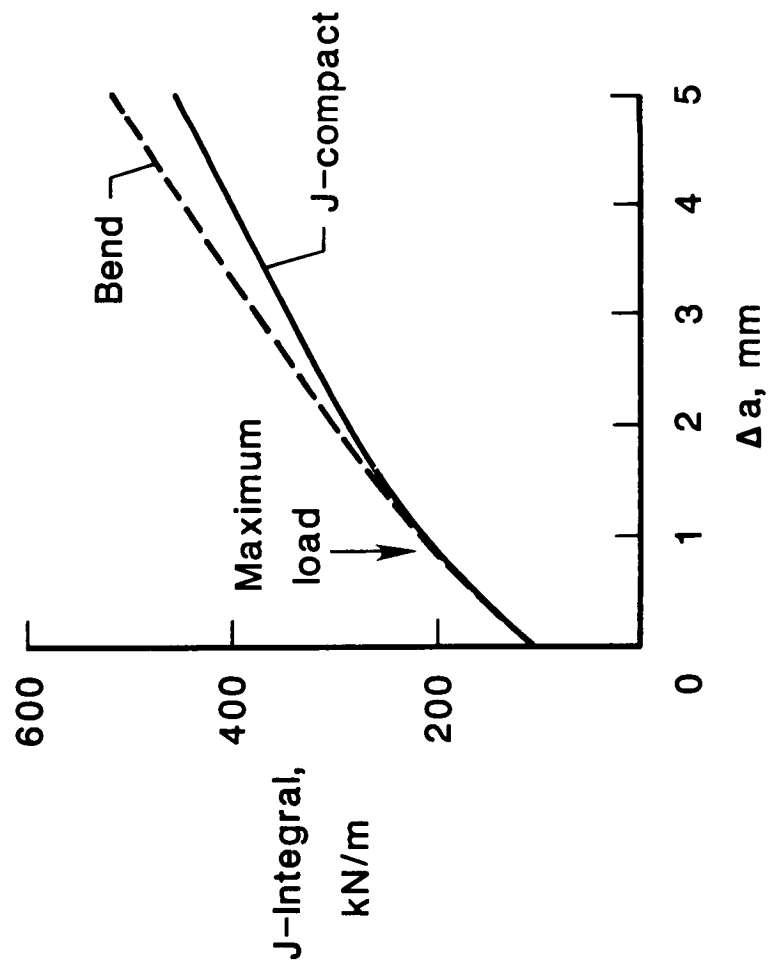


Figure 21.